

1 **Title: Diet gel-based oral drug delivery system for controlled dosing of small molecules**
2 **for microglia depletion and inducible Cre recombination in mice**

3

4 **Authors:** Joel Jovanovic^{1,2}, Megan L. Stone³, Samantha R. Dooyema^{1,2}, Yuankai K. Tao^{1,2,4},
5 Sabine Fuhrmann^{1,2,3}, Edward M. Levine^{1,2,3}

6

7 **Affiliation:** ¹ Vanderbilt Eye Institute, Vanderbilt University Medical Center, Nashville, TN,
8 United States, ² Department of Ophthalmology and Visual Sciences, Vanderbilt University,
9 Nashville, TN, United States, ³ Department of Cell and Developmental Biology, Vanderbilt
10 University, Nashville, TN, United States, ⁴ Department of Biomedical Engineering, Vanderbilt
11 University, Nashville, TN, United States

12

13 **Abstract:**

14 Small molecules like PLX5622 for microglia depletion and Tamoxifen for inducible Cre
15 recombination are commonly used in mouse research. Traditional application methods, such
16 as chow or oral gavage and injections, have limitations, including uncontrolled dosage and risk
17 of injury. To address this issue, we have developed an alternative oral drug delivery system
18 using a gel-based rodent maintenance diet that allows for controlled consumption and
19 adjustment of dosage and is suitable for water-insoluble small molecules. We tested DietGel®
20 93M (93M) infused with PLX5622 (0.8 mg/g and 2.0 mg/g) in the *Cx3cr1^{gfp/+}* retinal microglia
21 reporter mouse and Tamoxifen-infused 93M (0.3125 mg/g) in the *Rlbp1-Cre^{ERT2};Rosa^{ai14}*
22 mouse with an inducible tdTomato reporter in retinal Müller glia. Mice were single-caged and
23 received daily batches of PLX5622-infused 93M over 14 days or Tamoxifen-infused 93M for
24 one or three days followed by a 14-day observation period. Longitudinal scanning laser
25 ophthalmoscopy *in vivo* and fixed tissue imaging were used to track GFP and tdTomato
26 expression. Following evaluation of a suitable 93M consumption rate (g/d) to sustain body
27 weight, the PLX5622-93M diet at both concentrations showed a 94% microglia depletion rate
28 at 3 days and >99% after one and two weeks. The Tamoxifen-93M diet confirmed suitability for
29 inducible Cre recombination, with significant treatment-time dependent efficacy and a positive
30 correlation between total Tamoxifen dose and tdTomato expression. This study demonstrates

31 that a diet gel-based drug delivery system offers a controllable and less invasive alternative to
32 current drug application methods for PLX5622 and Tamoxifen.

33

34 **Keywords:** 3Rs, refinement, DietGel® 93M, gel-based rodent diet, drug delivery system, small
35 molecules, PLX5622, Tamoxifen, microglia, Müller glia, Cre recombination, scanning laser
36 ophthalmoscopy (SLO)

37

38 **Introduction:**

39 Over the past years, different drug delivery systems for rodents have been established in
40 biomedical research. The preferred route of delivery often depends on the drug's properties,
41 the drug vehicle, the required dose, and the rodent's condition ^{1,2}. Among the most used
42 systemic delivery methods using the oral route are gavage, drinking water or hydration gels,
43 and drug-infused chow, while other drugs require bypassing the first pass effect by using the
44 parenteral route, such as intravenous (tail vein), subcutaneous or intraperitoneal (i.p.)
45 injections ^{1,3-6}. Even though these systems are widely used, they have disadvantages that
46 must be considered such as the risk of injury, stress to the animal, and control over dosage.

47 Recently, a broad range of small molecules became available for a variety of purposes ^{7,8}.
48 Among commonly used small molecules in research are PLX5622 for microglia depletion and
49 Tamoxifen for CreER recombination ⁹⁻¹⁴. PLX5622 is a small molecule kinase inhibitor that
50 selectively blocks the CSF1R signaling required for cell survival in monocytes, and in microglia
51 and macrophages in the CNS ¹⁵. Tamoxifen is a selective estrogen receptor modulator widely
52 used in combination with a Cre recombinase-LoxP system for tissue-specific and temporal
53 gene regulation in mice ¹⁶⁻¹⁸.

54 Due to the water-insoluble properties of both drugs, the standard oral application methods
55 for these small molecules include drug-infused chow (ad libitum) for PLX5622 and Tamoxifen
56 or oral gavage for Tamoxifen. However, these methods may not always be suitable. While
57 chow lacks control over dosage (mg/g) and consumption rate (g/day) between rodents, oral
58 gavage risks injury and stress to the animals. Therefore, an alternative that mitigates these
59 effects is needed. In this study, we have developed a diet gel-based oral drug delivery system
60 that allows for dosage adjustment and is suitable for water-insoluble small molecules using the
61 complete gel-based maintenance diet ClearH₂O® DietGel® 93M (93M).

62

63 **Results:**

64 **A 93M DietGel® consumption rate of 8 g/day allows for complete consumption and**
65 **steady body weight**

66 To facilitate the transition from regular chow to diet gel and to allow for a time-matched start
67 of the experiment across all conditions, mice were fasted for 16 hours before the experimental
68 start. Body weight was tracked throughout the experiments with the post-fast body weight
69 serving as the baseline. This allowed us to directly assess the effect of the diet gel with and
70 without drug infusion.

71 As a first step, we determined the optimal daily consumption rate of drug-free 93M by
72 assigning three feeding groups to receive either 6, 8, or 10 grams per day (g/d) of 93M over 14
73 days (**Fig. 1a**). This experiment used B6129SF1/J mice which share the genetic background
74 with the two strains used for the following drug-incorporation studies. Body weight and the
75 residual amount of food (unconsumed 93M) were measured daily after each feeding cycle,
76 including a body weight measurement right before and after an initial fasting period of 16 hours
77 before the 93M feeding start. Each feeding group included 3 male and 3 female mice, and all
78 mice were single caged for the experiments.

79 **Fig. 1b** shows the mean amount of unconsumed food at each time point for males and
80 females. For both sexes, 6 and 8 g were completely consumed over the course of the
81 experiment except for one female on day 5. In contrast, unconsumed food was left behind
82 every day with 10 g/d. This shows that males and females consistently consume 6 or 8 g/d and
83 leave food behind when given 10g/d with an average of 0.86 ± 0.09 g/d for males and $1.14 \pm$
84 0.12 g/d for females without a significant difference between them ($P = 0.0588$, two-tailed
85 unpaired t-test).

86 A potential confound that could underestimate the amount of unconsumed food and lead to
87 miscalculation of an ingested drug dose is evaporation. Our temporal weight measuring data of
88 93M at 6 g, 8 g, and 10 g held in ventilated cages show mass reductions between 25% to 40%
89 over 24 hours, depending on the initial amount of 93M and on the drug-vehicle mix-in
90 (**Supplementary Fig. 1**). However, we observed that mice in the 6 g/d and 8 g/d groups did
91 not leave food residues in the petri dishes, indicating that they consumed the full portions. For

92 the 10 g/d group, however, the true mass of the unconsumed 93M could be greater than what
93 was measured due to the uncertainty of when the food was consumed over a 24-hour period.

94 To determine the effect of the three different provided amounts of 93M on body weight
95 maintenance, animals were weighed daily, and the measurements were normalized to the
96 initial post-fasting weights for each animal (day 0) (**Fig. 1c,d**). Two-way ANOVA shows that
97 both sexes have significant variations in body weight changes depending on the feeding
98 amount ($p_{\text{males}} < 0.0001$, $p_{\text{females}} < 0.0001$) and time ($p_{\text{males}} = 0.0036$, $p_{\text{females}} = 0.0013$). These
99 significant changes were specifically observed in mice given 6 g/d which caused significant
100 drops in body weights, with one male mouse removed from the study on day 12 due to a
101 weight loss greater than 30%.

102 Overall, both males and females fed 8 g/d of 93M showed a steady body weight over time
103 and completely consumed the daily portions. Therefore, we decided to use 8 g/d of 93M for the
104 following drug incorporation studies.

105

106 **Efficient retinal microglia depletion kinetics in mice treated with low and high dose**

107 **PLX5622-infused 93M DietGel®**

108 The feasibility and efficacy of PLX5622-infused 93M (PLX5622-93M) treatment were tested
109 in *Cx3cr1^{gfp/+}* microglia reporter mice split into a low (0.8 mg/g) and a high (2.0 mg/g) dosage
110 group with feedings of 8 g/d over 14 days (**Fig. 2a**). Body weights and unconsumed food were
111 measured daily. Both groups included 8 mice with 4 males and 4 females. Scanning laser
112 ophthalmoscopy (SLO) was used to visualize the microglia depletion kinetics *in vivo* at day 0
113 (pre-treatment baseline), 3, 7, and day 14. Endpoint histology in retinal whole mounts was
114 used to confirm the *in vivo* results.

115 SLO proved the feasibility of 93M as a drug delivery system for PLX5622, as evidenced by
116 the loss of GFP+ cells, the readout for microglia depletion (**Fig. 2b**). Surprisingly, both dosages
117 showed significant depletion by 3 days of treatment ($P < 0.0001$) with similar depletion kinetics
118 for both sexes (**Fig. 2c**). Animals treated with 0.8 mg/g showed a 93.6% reduction in microglia
119 at day 3, 98.5% at day 7, and 99.1% at day 14. Animals treated with 2.0 mg/g showed a 93.8%
120 reduction in microglia at day 3, 98.6% at day 7, and 99.3% at day 14.

121 Quantification of fixed retinal whole mount tissues on day 14 confirms these findings (**Fig.**
122 **2d,e**), with a depletion of 99.8% for the low dose and 99.9% for the high dose when compared

123 to the vehicle-treated control group. In alignment with the SLO findings on day 14, there is no
124 significant difference between both dosages over both sexes with an adjusted P -value of
125 0.9973, while both have a significant effect in comparison to the DMSO-93M control group ($P <$
126 0.0001) on day 14.

127 As expected, the consumption of the PLX5633-93M was complete throughout the
128 experiment, except for the first two feeding cycles in females (**Supplementary Fig. 2a**).
129 Interestingly, the females that received either dosage and the males treated with the low dose
130 regained their initial body weight over the treatment course, while the males treated with 2.0
131 mg/g stayed at the level of the post-fasting weight (**Supplementary Fig. 2b,c**). Consistent with
132 this, the males treated with the higher dose had significantly lower normalized body weights
133 from day 4 onwards compared to the other treatment groups (**Supplementary Fig. 2d**). These
134 observations reveal a specific dose-dependent effect of PLX5622 in male mice that extends
135 beyond microglia depletion (see Discussion).

136 To exclude potential effects on the microglia counts caused by the drug vehicle DMSO in
137 the 93M, a separate SLO imaging session was conducted with 93M infused with DMSO only
138 (**Supplementary Fig. 2e**). The mice received 8 g daily feedings of DMSO-infused 93M and
139 were imaged at day 0 (pre-treatment) and on days 7 and 14 of the treatment. The microglia
140 counts in the *in vivo* images show in comparison to the pre-treatment condition ($578.50 \pm$
141 11.49) no effect on the total number of microglia present on day 7 (573.25 ± 19.77 ; $P = 0.9963$,
142 one-way ANOVA with Dunnett's multiple comparisons test) and day 14 (586.75 ± 13.92 ; $P =$
143 0.9154 , one-way ANOVA with Dunnett's multiple comparisons test).

144

145 **Tamoxifen-infused 93M DietGel[®] treated mice successfully induce tdTomato expression** 146 **in retinal Müller glia**

147 To test for feasibility and control over the level of Cre recombination using Tamoxifen-infused
148 93M (Tamoxifen-93M), we used $R1bp1-Cre^{ERT2};Rosa^{ai14}$ mice, which express tdTomato in
149 Müller glia after Tamoxifen treatment^{19–21}. Two treatment groups were designed to test for
150 different Tamoxifen exposure times: one with a short (1-day treatment) and one with a long
151 exposure (3-day treatment) (**Fig. 3a**). All mice received 8 g of Tamoxifen-infused 93M per day
152 of treatment with a Tamoxifen concentration in the food of 312.5 $\mu\text{g/g}$. This daily dose is
153 approximately equivalent to a single dose of 100 $\mu\text{g/g}$ body weight by oral gavage in a mouse

154 that weighs 25 g. Each group included 8 mice with 4 males and 4 females. Longitudinal SLO
155 imaging was performed to detect Cre-dependent tdTomato expression induction in retinal
156 Müller glia. Baseline expression levels were established before treatment began. Both groups
157 were followed up 7- and 14-days post-Tamoxifen treatment, including a 1-day post-treatment
158 time point for the 1-day treatment group. Endpoint histology was used to confirm the tdTomato
159 expression levels in fixed retinal whole mounts on day 14.

160 SLO confirmed successful Tamoxifen delivery and Cre recombination, as shown by the
161 induction of tdTomato expression over time (**Fig. 3b**). Interestingly, the 1-day treatment
162 showed a significant increase ($P < 0.0001$) in the tdTomato expression for males and females
163 after 24 hours, with a relative expression increase from $0.12\% \pm 0.04\%$ to $3.39\% \pm 0.45\%$ and
164 $0.14\% \pm 0.03\%$ to $3.29\% \pm 0.21\%$, respectively (**Fig. 3c**). The expression continued to
165 increase until the end of the experiment on day 14 to $21.35\% \pm 0.88\%$ for the males, and to
166 $22.09\% \pm 0.98\%$ for the females, without a significant difference between both sexes. The 3-
167 day treatment on day 14 caused a small but significant increase in tdTomato expression
168 compared to the 1-day treatment with a relative value of $27.78\% \pm 0.86\%$ for the males ($P =$
169 0.007) and $27.05\% \pm 1.12\%$ for the females ($P < 0.0001$) (**Fig. 3c**). No significant difference
170 was observed between both sexes within the same treatment regimes.

171 The endpoint evaluation of the expression level in the whole mounted retina supports the
172 treatment-time-dependent effect shown by the *in vivo* findings (**Fig. 3d,e**). The calculated
173 overall tdTomato expression for males and females following the 1-day treatment is $19.38\% \pm$
174 1.72% and $29.31\% \pm 1.76\%$ for the 3-day treatment, with a significant difference between
175 treatment times ($P = 0.0010$).

176 To control for potential effects caused by the corn oil (drug vehicle) in 93M, a separate SLO
177 study was conducted using the 3-day treatment paradigm with corn oil-infused 93M
178 (**Supplementary Fig. 3a**). The mice were imaged pre-treatment (baseline) and at days 7 and
179 14 post-treatment. The evaluation of the tdTomato expression *in vivo* showed no significant
180 differences at both time points when compared to the baseline conditions, with a relative
181 expression of $0.13\% \pm 0.04\%$ at baseline, and $0.09\% \pm 0.03\%$ and $0.10\% \pm 0.01\%$ on day 7
182 and 14, respectively. In comparison, the endpoint evaluation of the whole mounted retina
183 showed an average expression of $0.02\% \pm 0.01\%$ (**Fig. 3e**).

184 Unlike for the PLX5622-93M feeding, Tamoxifen in 93M caused variations in the
185 consumption rate between animals, with a tendency for females to leave more unconsumed
186 Tamoxifen-93M after each feeding cycle (**Supplementary Fig. 3b**), but without significant body
187 weight changes during the short treatment periods in comparison to the post-fasting conditions
188 (**Supplementary Fig. 3c,d**). Since the difference in consumption could result in differences in
189 Tamoxifen dosages between animals, a dose-response curve was calculated using a simple
190 linear regression analysis of the total dose for each animal versus the tdTomato expression
191 present in the retinal whole mounts on day 14 (**Fig. 4**). The total Tamoxifen dose per mouse
192 ($\mu\text{g/g}$ body weight) was calculated by the total amount (g) of consumed Tamoxifen-93M and
193 the averaged body weights over the treatment time (1 or 3 days). Both treatment groups show
194 a significant correlation between the dose and the tdTomato expression with an R^2 of 0.5686
195 for the 1-day treatment and R^2 of 0.6430 for the 3-day treatment.

196

197 **Discussion:**

198 Gel-based diets are often used to supplement chow for breeding purposes or in post-
199 operative or compromised animals to prevent body weight loss^{22–28}. However, gel-based
200 maintenance diets can also be used to fully replace chow^{29,30}. In this study, we identified that
201 daily feedings of 8 g of 93M per mouse is a suitable amount that can be completely consumed
202 and allows for steady body weight over time in adult mice of both sexes. Feeding a lower
203 amount, namely 6 g/d, caused a steady drop in body weight which was more pronounced in
204 males. This may be attributed to the higher average body weight of males with a mean
205 difference between the sexes of $32.8\% \pm 2.1\%$ on post-fast day 0 ($P < 0.0001$, unpaired two-
206 tailed t-test). On the other hand, the 93M consumption data of age-matched mice indicates that
207 females in the 10 g/d group tend, even though not significantly, to leave more unconsumed
208 food after each feeding cycle than their male counterparts.

209 Furthermore, we show that the gel texture and the liquefaction properties of 93M upon
210 heating allow for a simple way to infuse water-insoluble drugs into 93M. Here, we tested the
211 two small molecules, PLX5622 and Tamoxifen, with good results, and it is likely that this
212 delivery system could work for other water-insoluble drugs or test compounds.

213 Unexpectedly, our PLX5622 experiment using the high dose of 2.0 mg/g revealed a
214 significant dose-dependent effect on the body weights in male mice. This is a new and

215 interesting observation that may imply sex-specific metabolic changes in males upon high-
216 dose PLX5622 treatment, especially since PLX5622 has been shown to affect glucose
217 metabolism and adipose tissue remodeling^{31,32}. This should be considered for studies in which
218 a comparable dose is planned.

219 There are several advantages of using PLX5622-infused 93M for microglia depletion. This
220 approach enables the use of different drug concentrations with consistent consumption rates
221 over time in age-matched mice of both sexes. Another is the ability to easily and cost-
222 effectively adjust dosage in small batches of food. These features make it practical to test
223 PLX5622 from different vendors or between different production lots and adjust dosages
224 accordingly, which is cost-prohibitive with chow-based preparations. Another advantage is the
225 lower sucrose content of the AIN-93-based diet used here, which mainly uses corn starch as a
226 carbohydrate source, compared to the commonly used high sucrose-based AIN-76A chow for
227 PLX5622 and other drugs^{33,34}. In addition, the presented drug delivery system avoids the risks
228 and animal welfare concerns of invasive methods of PLX5622 applications, such as i.p.
229 injections of PLX5622-DMSO mixtures, which require daily injections^{35,36}. This method may be
230 suitable for bigger rodents, such as Sprague Dawley rats, but we observed abdominal cyst
231 formations during a trial of repeated PLX5622-DMSO i.p. injections into mice following a
232 published protocol³⁵. Overall, the diet gel-based delivery of PLX5622 is highly efficient,
233 mitigates adverse effects of other treatment routes, and allows for long-term exposure
234 experiments or the testing of different batches of drugs with adjusted dosages.

235 We also demonstrate that Tamoxifen can be infused into 93M and that feeding it to adult
236 and sex-matched mice induces Cre recombination. Here, a single Tamoxifen concentration
237 (312.5 µg/g) and a daily feeding amount (8 g/day) were used while controlling for the treatment
238 time (1-day vs. 3-day treatment). The longitudinal SLO data observing Cre-dependent
239 tdTomato expression in retinal Müller glia shows that Tamoxifen works quickly, with tdTomato
240 activation within 24 hours after one feeding cycle. Furthermore, the control over treatment time
241 is sufficient to significantly adjust the level of Cre recombination, despite the differences in
242 consumption between animals. An alternative to better control the level of Cre recombination
243 may be adjusting the Tamoxifen concentration in 93M to the individual body weights of the
244 mice. However, there might be a limitation on the amount of Tamoxifen that can be
245 incorporated due to palatability. Our data shows that mice show some reluctance to Tamoxifen-

246 infused 93M, which is more pronounced in females compared to male mice. Interestingly,
247 studies using a commercially available Tamoxifen-incorporated chow reported similar
248 observations with reduced feeding and weight loss within the first days of treatment^{37–39}. In our
249 study, we only observed a limited drop in body weight over the short treatment periods of one
250 and three days relative to the preceding post-fasting body weight (**Supplementary Fig. 3c,d**).
251 Interestingly, mice treated with 93M or corn oil-infused 93M also showed a limited initial weight
252 loss (**Fig. 1c,d** and **Supplementary Fig. 4a**), while this was not observed in the PLX5622-93M
253 or DMSO-infused 93M treated mice (**Supplementary Fig.2c,d**, and **Supplementary Fig. 4b**)
254 Thus, it remains unclear whether Tamoxifen, the switch to a gel-based diet, the mouse strain,
255 or a combination of these factors contributes to the weight loss. Overall, a high level of
256 recombination can be achieved with a repeated feeding regimen, whereas a single feeding can
257 be advantageous for mosaic recombination. Importantly, Tamoxifen-infused 93M offers a
258 refinement over gavage- or injection-based delivery.

259 In conclusion, our study shows that a gel-based diet such as 93M can be used as an
260 alternative system for dosage-controlled drug delivery. It shows the advantage of staying within
261 the balance of animal welfare concerns by minimizing injury, pain, or discomfort, and largely
262 staying within the boundaries of gaining or losing body weight of ± 25 percent, which could be
263 reduced by shortening fasting times. Furthermore, it allows for the preparation of small batches
264 in the lab, and therefore provides the ability to test or titrate new batches of drug. This diet gel-
265 based oral drug delivery system may also be expanded to other drugs that are water soluble or
266 water insoluble.

267

268 Limitations of approach:

269 93M liquification requires heating at 60°C which could inactivate heat-labile molecules
270 during incorporation. Another limitation may be the difficulty of increasing dosages in 93M if the
271 animals avoid the drug-infused diet due to palatability issues.

272

273 Limitations of study:

274 The consumption behavior was not recorded. Differences between animals could change
275 the outcomes depending on how quickly or slowly the animals eat the drug-infused 93M.

276 Furthermore, the optimal daily consumption amount of 93M was defined for 8–12-week-old

277 mice and may differ for other age groups. Another limitation is that we only investigated the
278 effect of drug-infused 93 M in the retina using one Cre line and a microglia reporter line. The
279 effectiveness of the drugs could differ in other tissues or in combination with different Cre or
280 reporter lines.

281

282 **Methods:**

283 Animals:

284 For all experiments, mice were single-caged, and sex- and age-matched (between 8 and
285 12 weeks). Mice were maintained in a temperature and humidity-controlled animal facility in
286 individually ventilated cages on a 12-hr light–dark schedule. All animals had access to food
287 according to the experimental design and to water ad libitum. Prior to each experiment mice
288 were deprived of food for 16 hours to increase appetite for a timely start of the experiment
289 across all experimental animals and to reduce eventual reluctance of 93M consumption due to
290 taste changes.

291 The study included three mouse strains: B6129SF1/J mice (RRID:IMSR_JAX:101043; The
292 Jackson Laboratory, ME, USA), which were used for the evaluation of the optimal daily
293 consumption rate of 93M. The *Cx3cr1^{gfp/+}* microglia reporter mice (B6.129P2(Cg)-*Cx3cr1*
294 *tm1^{Litt}/J*; RRID:IMSR_JAX:005582, The Jackson Laboratory, ME, USA) were used for the
295 PLX5622 study. The *Rlbp1-Cre^{ERT2};Rosa^{ai14}* mice (Gt(ROSA)26Sor^{tm14(CAG-tdTomato)Hze} Tg(*Rlbp1-*
296 *cre/ERT2*)1Eml/Eml; RRID:MGI:7708085; Levine Lab, VUMC, TN, USA) were used for the
297 Tamoxifen study^{19,20,40}. This study was approved by the Vanderbilt University Medical Center
298 Institutional Animal Care and Use Committee and conformed to the Association for Research
299 in Vision and Ophthalmology Statement for the Use of Animals in Ophthalmic and Vision
300 Research.

301

302 Experimental groups:

303 Three experiments were designed. The first experiment evaluated the optimal daily
304 consumption rate of 93M to ensure complete consumption while maintaining body weight by
305 testing a low (6 g), an intermediate (8 g), and a high amount (10 g) of 93M provided daily in
306 single-caged mice. The second tested the feasibility of PLX5622-infused 93M feeding as a
307 dosage-controllable method to deplete microglia at a low (0.8 mg/g) and a high (2.0 mg/g)

308 concentration. The third experiment tested whether Tamoxifen can be administered through
309 93M feeding at a single concentration (312.5µg/g) while controlling for the degrees of Cre
310 recombination by adjusting the duration of the treatment (1 versus 3-day treatment).

311

312 DietGel®:

313 Three different DietGel® products provided by ClearH₂O®, Inc., ME, USA were tested for
314 drug-vehicle incorporation, which included DietGel® Boost, DietGel® 93M, and DietGel® GEM.

315 DietGel® 93M (93M), a complete maintenance diet with enhanced flavor to promote
316 consumption (<https://clearh2o.com/products/dietgel%C2%AE-93m>, accessed on November
317 26th, 2024), was selected for the study based on smoothness, liquefaction properties upon
318 heating, and emulsion properties of oil-based additives.

319

320 PLX5622 and Tamoxifen incorporation into DietGel® 93M:

321 PLX5622 (C-1521, Lot#21; Chemgood, LLC., VA, USA) and Tamoxifen (T5648, Sigma-
322 Aldrich, MO, USA) were separately incorporated into 93M per cup. Each cup contains 75g of
323 93M (measured in our lab).

324 PLX5622 was incorporated at two different concentrations to a final concentration of 0.8
325 mg/g and 2.0 mg/g. For the initial concentration, 60 mg of PLX5622 and 150 mg for the latter
326 were each mixed into 1 ml of 100% DMSO (pharma grade, Heiltropfen Lab. LLP, UK) using a
327 1.5 ml microcentrifuge tube. The tubes were protected from light and placed on a rocker for
328 constant rocking for 1 hour at room temperature, followed by a 20-minute ultrasonic bath to
329 achieve complete dissolution.

330 Tamoxifen was used at a concentration of 312.5 µg/g. For one cup of 93M, 23.44 mg of
331 Tamoxifen was dissolved in 1 ml of corn oil (C8267, Sigma-Aldrich, MO, USA) on a rocker at
332 room temperature overnight (light protected).

333 Each cup of 93M was heated in a water bath at 60°C for 15 minutes to liquify 93M. 1ml of
334 the freshly prepared drug-vehicle solution was stirred in dropwise over 5 minutes using a
335 P1000 pipet and a metal spatula, followed by 5 min of stirring to achieve a homogenous
336 mixture. The cups were sealed with parafilm and placed on ice for 10 minutes before light-
337 protected storage at 4°C. The drug-infused 93M can be stored for at least up to one week at
338 4°C.

339 To measure out the desired amount of DietGel[®] for the experiment, a wooden single-use
340 spatula was used to transfer it into a 5 cm glass petri dish, which was then placed into the
341 mouse cage. The dishes were thoroughly cleaned out daily with paper towels before new food
342 was added.

343

344 Anesthesia and scanning laser ophthalmoscopy (SLO):

345 The custom-built multimodal MURIN system, including a 2-channel fluorescence SLO, was
346 used for *in vivo* retinal fluorescence imaging⁴¹. Mice were anesthetized using a mixture of
347 isoflurane and oxygen set at a ratio of 2.5% and a flow rate of 1.5 l/min. Mydriasis was induced
348 by applying 1-2 drops of 1% Tropicamide eye drops (VUMC pharmacy, Nashville, TN, USA).
349 The eyes were fitted with a custom zero-diopter contact lens to reduce optical aberrations at
350 the air-cornea interface⁴¹. During imaging, 0.3% hydroxypropyl methylcellulose lubricant eye
351 gel (GenTeal[®] Tears; Alcon) was periodically applied to preserve corneal hydration. Animals
352 were placed onto a custom water-heated imaging bed maintained at 38°C with an integrated
353 palate bar and nose cone to maintain anesthesia and reduce movement during the SLO
354 imaging session. The green channel was used to image the GFP signal in the microglia-
355 reporter mice B6.129P2(Cg)-Cx3cr1^{tm1Litt/J}, and the red channel for the tdTomato expression
356 in Müller glia of the Rbp1-Cre^{ERT2};Rosa^{ai14} mice. Each SLO scan consisted of 200 acquired
357 frames. Raw images were pre-processed as described elsewhere⁴¹.

358

359 Quantification of longitudinal microglia counts and relative tdTomato expression *in vivo* in SLO 360 scans:

361 Pre-processed SLO images were loaded into Fiji (ImageJ 1.54f, National Institutes of
362 Health) and twenty to thirty consecutive frames with minimal motion were selected for
363 averaged intensity orthogonal projection. The projection image was converted to an 8-bit
364 image followed by background subtraction with the rolling bar radius set at 20 pixels. The
365 images were further processed for noise reduction and therefore sharpening using the unsharp
366 mask function with a radius set at 6 pixels and a mask weight of 0.6 for the green channel
367 (GFP) and 0.3 for the red channel (tdTomato), respectively^{42,43}. A threshold was applied using
368 the threshold function 'Moments'. If needed, the threshold was manually adjusted to eliminate
369 background noise. The ROI manager was used to outline the entire field of view, and the area

370 fraction of positive pixels (% area) was automatically measured using the ‘Measure’ function
371 after selecting ‘Limit to threshold’ and ‘Area fraction’ in the measurement settings. The area
372 fraction is the relative tdTomato expression.

373
374 Retinal whole mount preparation and fluorescence microscopy:

375 All mice were euthanized at the end of each experiment for endpoint histology using CO₂
376 asphyxiation and secondary cervical dislocation. Both eyes were dissected using ophthalmic
377 micro-scissors and rinsed in 1x PBS. The eyes were fixed in 4% PFA overnight at 4°C. The left
378 eye was used for retinal whole-mount preparation. In brief, the cornea and lens were removed
379 using ophthalmic micro-scissors. The sclera along with the choroid and RPE were cut radially
380 and peeled off to expose the retina and subsequently separated by cutting the optic nerve at
381 its head. Next, four radial incisions were made into the retina before mounting on a glass slide
382 with the ganglion cell layer facing up. The whole mounts were coverslipped using Fluoromount-
383 G™ Mounting Medium (Invitrogen) and stored protected from light at 4°C upon imaging.

384 The retinal whole mounts were scanned with a ZEISS Axio Zoom.V16 with Apotome 3
385 microscope at 40X digital magnification using a 1x objective. A 4x4 tile scan was performed to
386 cover the entirety of the retina with a Z-stack interval set at 9 µm. The scanning depth was
387 individually adjusted to include all signal-positive layers. Apotome images were created using
388 the software's internal image processing function, and tiles were fused with an overlap set at
389 20%.

390
391 Endpoint quantification of microglia and relative tdTomato expression in retinal whole mounts

392 Apotome images were loaded into Fiji (ImageJ 1.54f, National Institutes of Health) for
393 maximum intensity orthogonal projection. The projection image was converted to an 8-bit
394 grayscale image. The background was subtracted with the rolling bar radius set at 50 pixels. A
395 retinal ROI (rROI) outlining the retina without including the optical nerve head was created and
396 saved by subtracting the optic nerve head area from the retinal area using the XOR function in
397 the ROI manager. Next, separate image analysis protocols were used for images showing
398 GFP-expressing microglia and tdTomato expressing Müller glia.

399 Microglia reporter images were filtered using the morphological filtering operation ‘Top-hat’
400 with a radius set at 3 pixels to homogenize the background and enhance the morphological

401 boundaries (contrast enhancement) for accurate automated cell counting^{44–47}. A threshold was
402 defined using the ‘Otsu’ settings and manually adjusted if needed. The ‘Analyze particles’
403 function was used for automated counting of individual cell bodies within the rROI. To do so,
404 the size (micron²) was set to 10 – infinity, and ‘Count Masks’ and ‘Add to Manager’ were
405 selected. The output files included ROIs of each counted cell. The new ROIs were overlaid
406 onto the original image to confirm proper cell counting. If inaccurate, the counting was
407 repeated with an adjusted threshold.

408 For the images showing tdTomato expressing whole mounts, a threshold was defined using
409 the function ‘Moments’ and, if necessary, manually adjusted to improve the background-to-
410 signal ratio. To confirm proper thresholding, the function ‘Create Selection’ was used to create
411 an ROI outlining all positive pixels, which was then pasted onto the original image. The
412 threshold was adjusted if the selection was deemed inaccurate. The rROI was applied to the
413 threshold image before the ‘Measure’ function was used to calculate the area fraction (% area)
414 of tdTomato positive pixels within the rROI. The area fraction is the relative tdTomato
415 expression in the retinal whole mounts.

416

417 Statistics:

418 The GraphPad Prism 10.4.1 software (GraphPad Software, Inc., La Jolla, CA, USA) was
419 used for data visualization and statistical analysis. Results are shown as Mean ± SEM. A *P*-
420 value below 0.05 was considered significant.

421

422 **Data availability**

423 The data generated during the current study are available from the corresponding authors
424 upon request.

425

426 **Acknowledgments:**

427 We thank the members of the Levine and Fuhrmann laboratories for their insights and support
428 during the course of this project.

429

430 **Disclosures:**

431 The authors declare the following competing interests: DietGel[®] 93M was provided by
432 ClearH₂O[®], Inc., ME, USA. PLX5622 was provided at a discount by Chemgood, LLC., VA,
433 USA. These companies or their representatives had no role in the study's design,
434 implementation, or interpretation and reporting of the results.

435

436 **Funding:**

437 NIH Grants: R21-EY033471, P30-EY008126, the 2023 Loris and David Rich Postdoctoral
438 Scholar Award from the International Retinal Research Foundation, the William A. Black Chair
439 in Ophthalmology, and unrestricted funds to the Department of Ophthalmology & Visual
440 Sciences from Research to Prevent Blindness, Inc.

441

442 **References:**

- 443 1. Turner, P. V, Pekow, C., Vasbinder, M. A. & Brabb, T. Administration of substances to
444 laboratory animals: equipment considerations, vehicle selection, and solute preparation.
445 *J Am Assoc Lab Anim Sci* **50**, 614–27 (2011).
- 446 2. Gad, S. C. *et al.* Tolerable Levels of Nonclinical Vehicles and Formulations Used in
447 Studies by Multiple Routes in Multiple Species With Notes on Methods to Improve Utility.
448 *Int J Toxicol* **35**, 95–178 (2016).
- 449 3. Anselmo, A. C., Gokarn, Y. & Mitragotri, S. Non-invasive delivery strategies for biologics.
450 *Nat Rev Drug Discov* **18**, 19–40 (2019).
- 451 4. Jain, K. K. An Overview of Drug Delivery Systems. in *Methods in molecular biology*
452 (*Clifton, N.J.*) vol. 2059 1–54 (2020).
- 453 5. Hovard, A., Teilmann, A., Hau, J. & Abelson, K. The applicability of a gel delivery system
454 for self-administration of buprenorphine to laboratory mice. *Lab Anim* **49**, 40–45 (2015).
- 455 6. Overk, C. R., Borgia, J. A. & Mufson, E. J. A novel approach for long-term oral drug
456 administration in animal research. *J Neurosci Methods* **195**, 194–199 (2011).
- 457 7. Zhong, L. *et al.* Small molecules in targeted cancer therapy: advances, challenges, and
458 future perspectives. *Signal Transduct Target Ther* **6**, 201 (2021).
- 459 8. Beck, H., Härter, M., Haß, B., Schmeck, C. & Baerfacker, L. Small molecules and their
460 impact in drug discovery: A perspective on the occasion of the 125th anniversary of the
461 Bayer Chemical Research Laboratory. *Drug Discov Today* **27**, 1560–1574 (2022).
- 462 9. Spangenberg, E. *et al.* Sustained microglial depletion with CSF1R inhibitor impairs
463 parenchymal plaque development in an Alzheimer’s disease model. *Nat Commun* **10**,
464 3758 (2019).
- 465 10. Ebnetter, A., Kokona, D., Jovanovic, J. & Zinkernagel, M. S. Dramatic Effect of Oral CSF-
466 1R Kinase Inhibitor on Retinal Microglia Revealed by In Vivo Scanning Laser
467 Ophthalmoscopy. *Transl Vis Sci Technol* **6**, 10 (2017).
- 468 11. Jovanovic, J., Liu, X., Kokona, D., Zinkernagel, M. S. & Ebnetter, A. Inhibition of
469 inflammatory cells delays retinal degeneration in experimental retinal vein occlusion in
470 mice. *Glia* **68**, 574–588 (2020).
- 471 12. Wickel, J. *et al.* Repopulated microglia after pharmacological depletion decrease
472 dendritic spine density in adult mouse brain. *Glia* **72**, 1484–1500 (2024).
- 473 13. Park, E. J. *et al.* System for tamoxifen-inducible expression of cre-recombinase from the
474 *Foxa2* locus in mice. *Developmental Dynamics* **237**, 447–453 (2008).

- 475 14. Jardí, F. *et al.* A shortened tamoxifen induction scheme to induce CreER recombinase
476 without side effects on the male mouse skeleton. *Mol Cell Endocrinol* **452**, 57–63 (2017).
- 477 15. Elmore, M. R. P. *et al.* Colony-Stimulating Factor 1 Receptor Signaling Is Necessary for
478 Microglia Viability, Unmasking a Microglia Progenitor Cell in the Adult Brain. *Neuron* **82**,
479 380–397 (2014).
- 480 16. Ichise, H. *et al.* Establishment of a tamoxifen-inducible Cre-driver mouse strain for
481 widespread and temporal genetic modification in adult mice. *Exp Anim* **65**, 231–244
482 (2016).
- 483 17. Navabpour, S., Kwapis, J. L. & Jarome, T. J. A neuroscientist’s guide to transgenic mice
484 and other genetic tools. *Neurosci Biobehav Rev* **108**, 732–748 (2020).
- 485 18. Chen, M.-Y., Zhao, F.-L., Chu, W.-L., Bai, M.-R. & Zhang, D.-M. A review of tamoxifen
486 administration regimen optimization for Cre/loxP system in mouse bone study.
487 *Biomedicine & Pharmacotherapy* **165**, 115045 (2023).
- 488 19. Stone, M. L., Lee, H. H. & Levine, E. M. Agarose hydrogel-mediated electroporation
489 method for retinal tissue cultured at the air-liquid interface. *iScience* **27**, 111299 (2024).
- 490 20. Pollak, J. *et al.* ASCL1 reprograms mouse Müller glia into neurogenic retinal progenitors.
491 *Development* **140**, 2619–2631 (2013).
- 492 21. Webster, M. K. *et al.* Stimulation of Retinal Pigment Epithelium With an $\alpha 7$ nAChR
493 Agonist Leads to Müller Glia Dependent Neurogenesis in the Adult Mammalian Retina.
494 *Investigative Ophthalmology & Visual Science* **60**, 570 (2019).
- 495 22. Felgenhauer, J. L. *et al.* Evaluation of Nutritional Gel Supplementation in C57BL/6J Mice
496 Infected with Mouse-Adapted Influenza A/PR/8/34 Virus. *Comp Med* **70**, 471–486
497 (2020).
- 498 23. Gates, K. V, Alamaw, E., Jampachaisri, K., Huss, M. K. & Pacharinsak, C. Efficacy of
499 Supplemental Diet Gels for Preventing Postoperative Weight Loss in Mice (*Mus*
500 *musculus*). *Journal of the American Association for Laboratory Animal Science* **62**, 87–
501 91 (2023).
- 502 24. Wong, R. K. *et al.* Effects of Supplemental Diet during Breeding on Fertility, Litter Size,
503 Survival Rate, and Weaning Weight in Mice (*Mus musculus*). *Journal of the American*
504 *Association for Laboratory Animal Science* **63**, 480–487 (2024).
- 505 25. Froberg-Fejko, K. M. & Lecker, J. Overview and indications for use of Bio-Serv’s Nutra-
506 Gel diet for laboratory rodents. *Lab Anim (NY)* **40**, 326–327 (2011).

- 507 26. Wong, R. K. *et al.* Effects of Supplemental Diet during Breeding on Fertility, Litter Size,
508 Survival Rate, and Weaning Weight in Mice (*Mus musculus*). *Journal of the American*
509 *Association for Laboratory Animal Science* **63**, 480–487 (2024).
- 510 27. Young, M. S. *et al.* Subcutaneous Alfaxalone-Xylazine-Buprenorphine for Surgical
511 Anesthesia and Echocardiographic Evaluation of Mice (*Mus musculus*). *Journal of the*
512 *American Association for Laboratory Animal Science* **63**, 49–56 (2024).
- 513 28. Boatman, S. *et al.* Diet-induced shifts in the gut microbiota influence anastomotic healing
514 in a murine model of colonic surgery. *Gut Microbes* **15**, (2023).
- 515 29. Imamura, Y. *et al.* Ultrasound stimulation of the vagal nerve improves acute septic
516 encephalopathy in mice. *Front Neurosci* **17**, (2023).
- 517 30. Iban-Arias, R. *et al.* Ad-derived bone marrow transplant induces proinflammatory
518 immune peripheral mechanisms accompanied by decreased neuroplasticity and reduced
519 gut microbiome diversity affecting AD-like phenotype in the absence of A β
520 neuropathology. *Brain Behav Immun* **118**, 252–272 (2024).
- 521 31. Bosch, A. J. T. *et al.* CSF1R inhibition with PLX5622 affects multiple immune cell
522 compartments and induces tissue-specific metabolic effects in lean mice. *Diabetologia*
523 **66**, 2292–2306 (2023).
- 524 32. Ali, S. *et al.* CSF1R inhibitor PLX5622 and environmental enrichment additively improve
525 metabolic outcomes in middle-aged female mice. *Aging* **12**, 2101–2122 (2020).
- 526 33. Reeves, P. G., Nielsen, F. H. & Fahey, G. C. AIN-93 Purified Diets for Laboratory
527 Rodents: Final Report of the American Institute of Nutrition Ad Hoc Writing Committee on
528 the Reformulation of the AIN-76A Rodent Diet. *J Nutr* **123**, 1939–1951 (1993).
- 529 34. Reeves, P. G. Components of the AIN-93 Diets as Improvements in the AIN-76A Diet. *J*
530 *Nutr* **127**, 838S-841S (1997).
- 531 35. Riquier, A. J. & Sollars, S. I. Astrocytic response to neural injury is larger during
532 development than in adulthood and is not predicated upon the presence of microglia.
533 *Brain Behav Immun Health* **1**, 100010 (2020).
- 534 36. Riquier, A. J. & Sollars, S. I. Terminal field volume of the glossopharyngeal nerve in adult
535 rats reverts to prepruning size following microglia depletion with PLX5622. *Dev*
536 *Neurobiol* **82**, 613–624 (2022).
- 537 37. Andersson, K. B., Winer, L. H., Mørk, H. K., Molkentin, J. D. & Jaisser, F. Tamoxifen
538 administration routes and dosage for inducible Cre-mediated gene disruption in mouse
539 hearts. *Transgenic Res* **19**, 715–725 (2010).

- 540 38. Chiang, P.-M. *et al.* Deletion of *TDP-43* down-regulates *Tbc1d1* , a gene linked to
541 obesity, and alters body fat metabolism. *Proceedings of the National Academy of*
542 *Sciences* **107**, 16320–16324 (2010).
- 543 39. Miró-Murillo, M. *et al.* Acute Vhl gene inactivation induces cardiac HIF-dependent
544 erythropoietin gene expression. *PLoS One* **6**, e22589 (2011).
- 545 40. Vazquez-Chona, F. R., Clark, A. M. & Levine, E. M. Rlbp1 Promoter Drives Robust Müller
546 Glial GFP Expression in Transgenic Mice. *Investigative Ophthalmology & Visual Science*
547 **50**, 3996 (2009).
- 548 41. Rico-Jimenez, J. J. *et al.* MURIN: Multimodal Retinal Imaging and Navigated-laser-
549 delivery for dynamic and longitudinal tracking of photodamage in murine models.
550 *Frontiers in Ophthalmology* **3**, (2023).
- 551 42. Penazzi, L., Sündermann, F., Bakota, L. & Brandt, R. Machine Learning to Evaluate
552 Neuron Density in Brain Sections. in 263–291 (2014). doi:10.1007/978-1-4939-0381-
553 8_13.
- 554 43. Ogura, A., Hayakawa, K., Miyati, T. & Maeda, F. Improvement on detectability of early
555 ischemic changes for acute stroke using nonenhanced computed tomography: Effect of
556 matrix size. *Eur J Radiol* **76**, 162–166 (2010).
- 557 44. Li, J. *et al.* Segmentation of retinal microaneurysms in fluorescein fundus angiography
558 images by a novel three-step model. *Front Med (Lausanne)* **11**, (2024).
- 559 45. Bai, X., Zhou, F. & Xue, B. Image enhancement using multi scale image features
560 extracted by top-hat transform. *Opt Laser Technol* **44**, 328–336 (2012).
- 561 46. Bai, X., Zhou, F. & Xue, B. Toggle and top-hat based morphological contrast operators.
562 *Computers & Electrical Engineering* **38**, 1196–1204 (2012).
- 563 47. Ghislain, F., Beaudelaire, S. T. & Daniel, T. An accurate unsupervised extraction of retinal
564 vasculature using curvelet transform and classical morphological operators. *Comput Biol*
565 *Med* **178**, 108801 (2024).
- 566
- 567

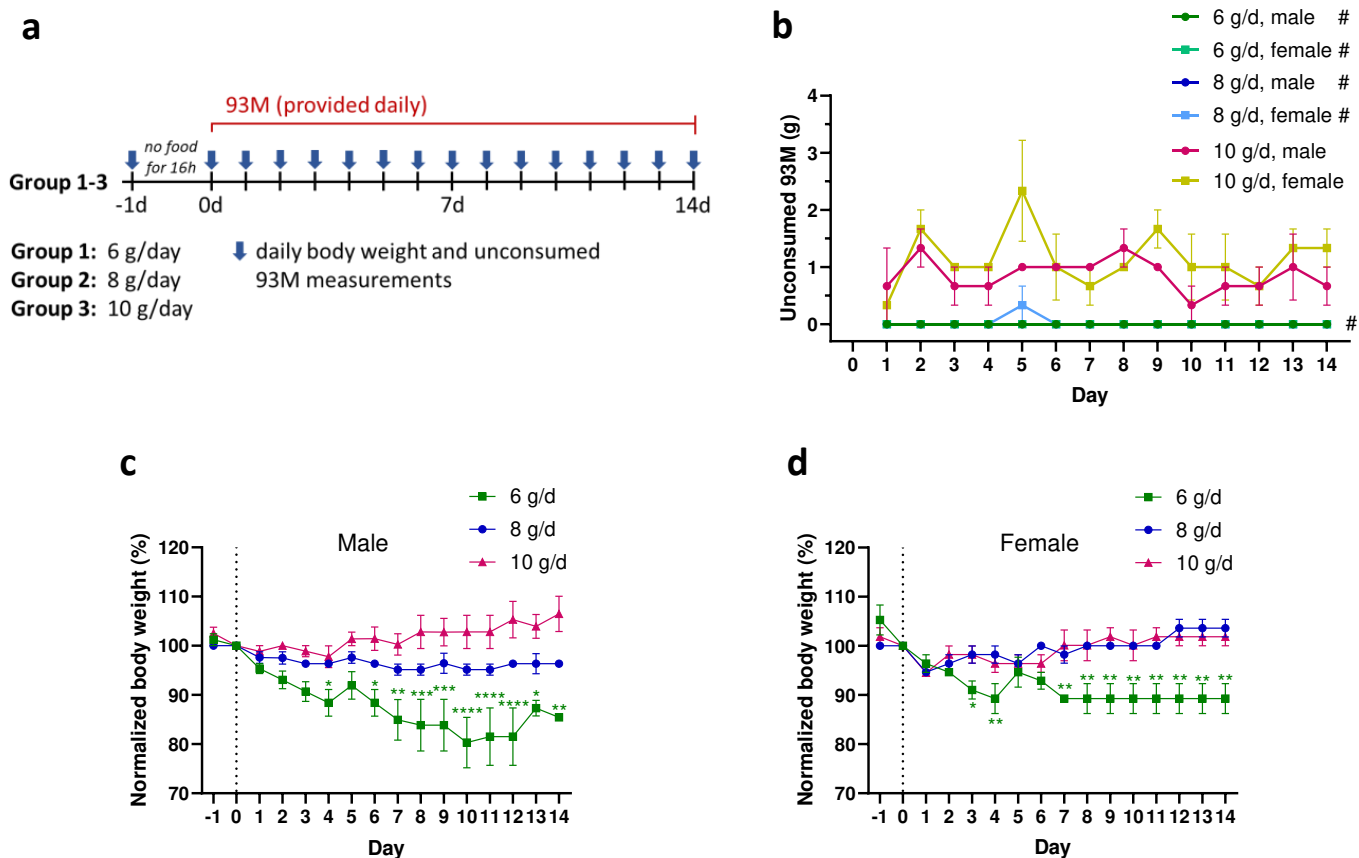


Fig. 1: Consumption rate determination for steady body weight and complete consumption of provided 93M in B6129SF1/J mice. a, Experimental design of feeding groups receiving either 6g, 8g or 10g of drug-free 93M every 24 hours over 14 days. Unconsumed 93M (g) and body weight (g) were measured after each 24h-feeding cycle, including a body weight measurement before (day -1) and after (day 0) an initial fasting period of 16 hours. **b,** Unconsumed 93M (g) after each feeding cycle per feeding group and sex. #: The data points are at 0 g of unconsumed 93M. **c,d,** Temporal body weight measurements normalized and compared to the post-fasting body weight (day 0) in males and females. N = 6 mice (3 males, 3 females) per feeding group. Statistics: Two-way ANOVA with Dunnett's multiple comparisons tests for (c,d). Results are shown as Mean \pm SEM. Significance levels: * $P < .05$, ** $P < .01$, *** $P < .001$, **** $P < .0001$.

Figure 2

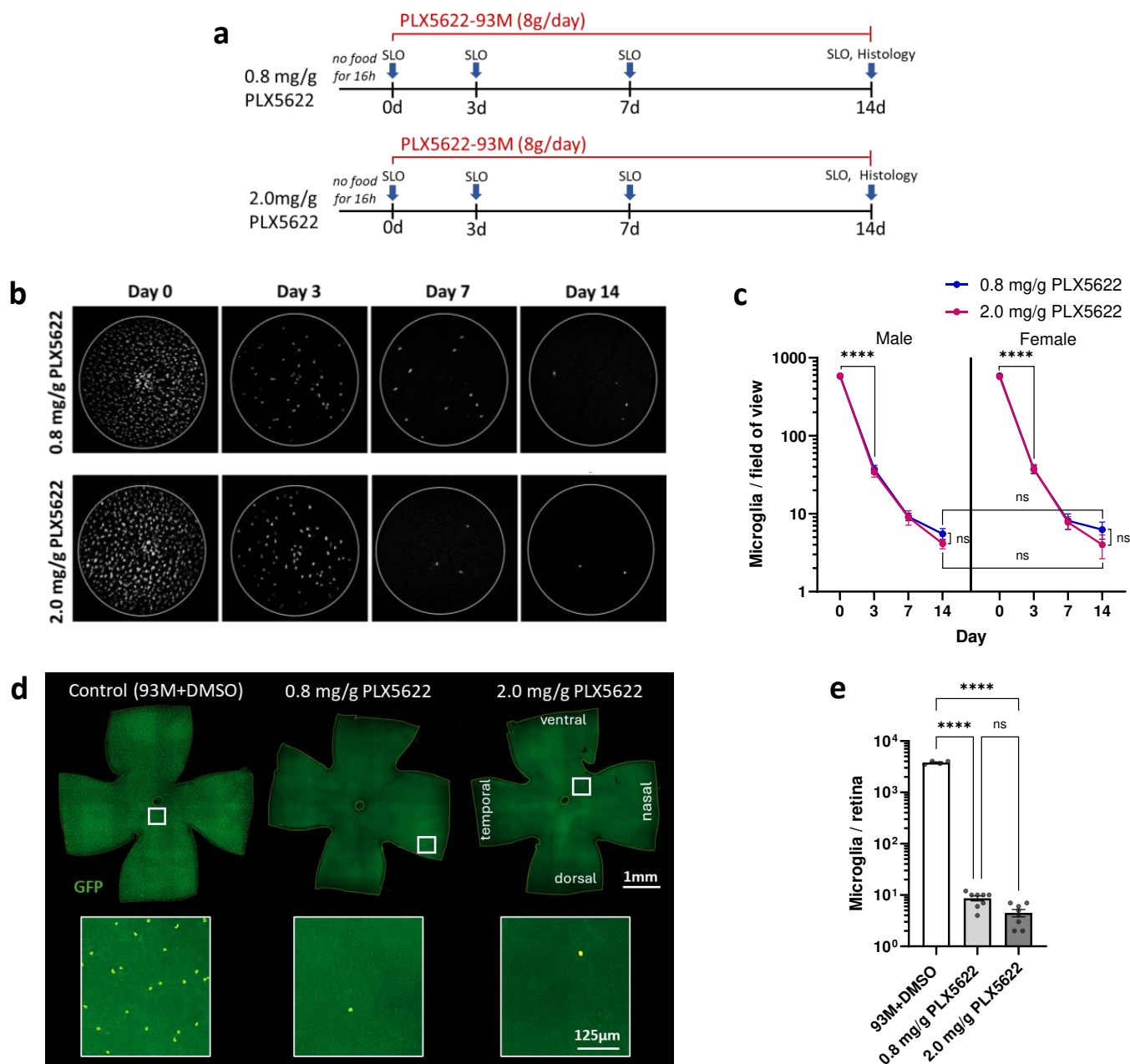


Fig. 2: Feasibility and efficacy evaluation of PLX5622-infused 93M for retinal microglia depletion in GFP expressing microglia reporter mice. **a**, Experimental design with two PLX5622-93M dosage groups (0.8 mg/g and 2.0 mg/g) in heterozygous B6.129P2(Cg)-*Cx3cr1*^{tm1Litt}/J mice receiving 8 g/d over 14 days, including daily body weight and unconsumed food measurements. SLO was performed on day 0, 3, 7, and 14. **b**, Representative longitudinal SLO image series per treatment group shows retinal microglia depletion *in vivo*. **c**, Quantification of microglia counts in SLO images per sex and dosage group. **d**, Representative endpoint histology (day 14) of whole mounted retina per dosage group, including a control retina treated with DMSO-infused 93M. The inset shows a magnified section with masked microglia (yellow boundary) for better visualization. **e**, Quantification of microglia counts in retinal whole mounts over both sexes per dosage group. N = 8 mice (4 males, 4 females) per PLX5622 dosage group. Statistics: Two-way ANOVA with Tukey's multiple comparisons test for (c) and one-way ANOVA with Tukey's multiple comparisons test for (e). The results are shown as Mean \pm SEM. Significance level: **** $P < .0001$.

Figure 3

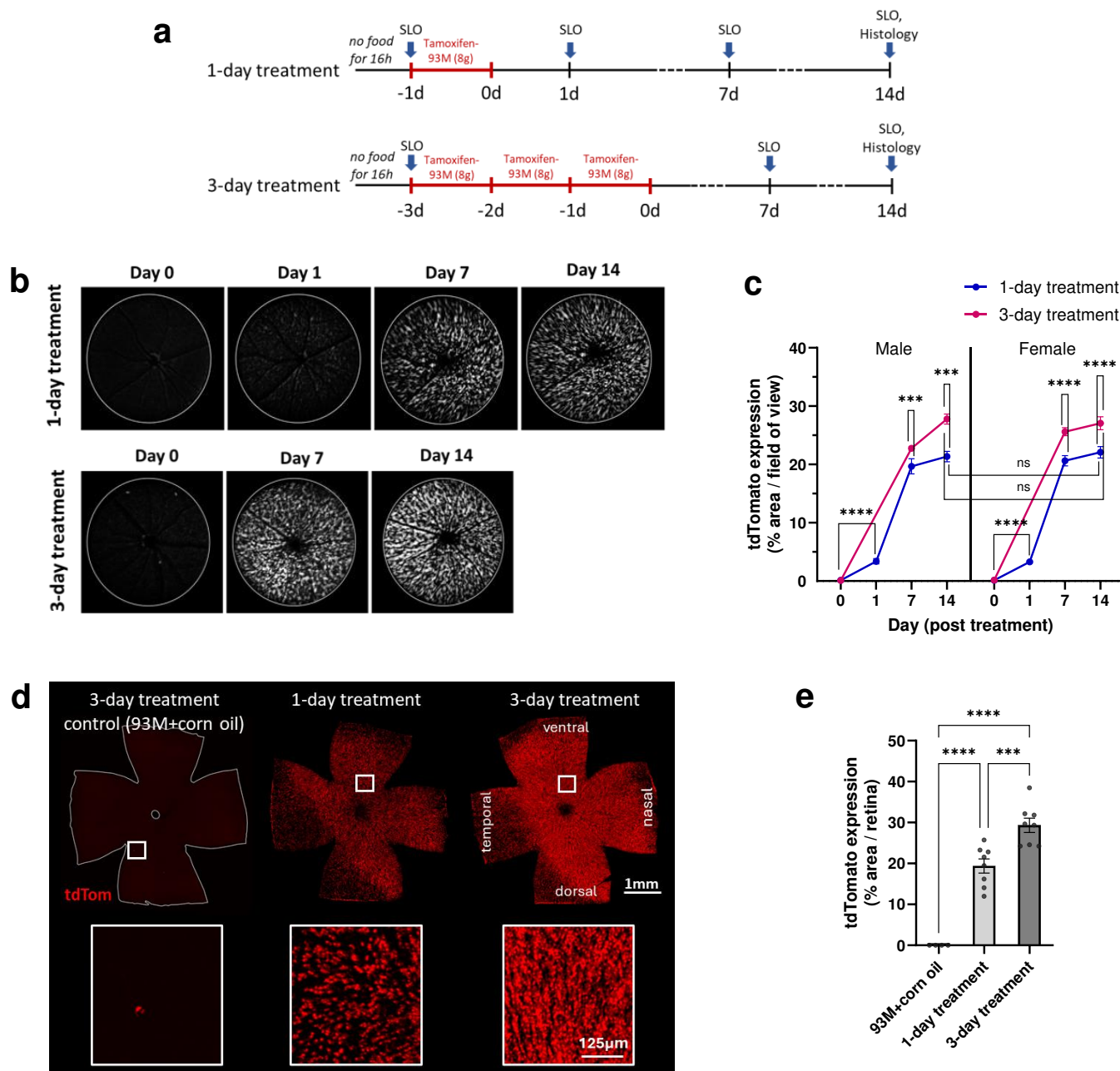


Fig. 3: Feasibility and efficacy evaluation of Tamoxifen-infused 93M for Cre recombination using a mouse line with inducible tdTomato expression in retinal Müller glia. **a**, Experimental design for 1-day and 3-day Tamoxifen-93M treatment groups in *Rlbp1-Cre^{ERT2};Rosa^{ai14}* mice. Both groups received 8 g/d with an equal Tamoxifen concentration of 312.5 $\mu\text{g/g}$. The body weight and unconsumed Tamoxifen-93M were measured after each feeding cycle. SLO was performed for the 1-day treatment on day -1, 0, 1, 7, and 14, and on day -3, 0, 7, and 14 for the 3-day treatment. **b**, Representative longitudinal SLO image series per treatment group shows tdTomato expression induction *in vivo*. **c**, Quantification of the TdTomato expression as an area fraction of positive pixels in SLO images per sex and treatment group. **d**, Representative endpoint histology (day 14) of whole mounted retina per treatment group, including a control retina treated with corn oil-infused 93M. The reduced tdTomato expression in the dorso-temporal area is a commonly observed feature in the *Rlbp1-Cre^{ERT2};Rosa^{ai14}* line upon Tamoxifen treatment and therefore not specific to the diet gel-based treatment approach. **e**, Quantification of tdTomato expression as an area fraction of positive pixels in retinal whole mounts over both sexes per treatment group. $N = 8$ mice (4 males, 4 females) per Tamoxifen treatment group. Statistics: Two-way ANOVA with Tukey's multiple comparisons test for (c) and one-way ANOVA with Tukey's multiple comparisons test for (e). Results are shown as Mean \pm SEM. Significance levels: *** $P < .001$, **** $P < .0001$.

